Clin. Lab. 2026;72:XXX-XXX

ORIGINAL ARTICLE

Nontargeted Metabolomics Analysis of Carbapenem-Resistant *Pseudomonas aeruginosa*

Yao Zhang [1, 2, *], Xiaona Yin [1, 2, *], Yanghu Xie [1, 3], Xiaoqiong Wang [1, 2], Yongsheng Wang [1, 2]

[*] *Co-first Authors: Yao Zhang, Xiaona Yin*
[1] *Department of Pulmonary and Critical Care Medicine, The Second People's Hospital of Hefei, Hefei Hospital Affiliated to Anhui Medical University, Hefei, Anhui, China*
[2] *Fifth Clinical Medical College of Anhui Medical University, Hefei, Anhui, China*
[3] *Department of Medical Laboratory Medicine, The Second People's Hospital of Hefei, Hefei Hospital Affiliated to Anhui Medical University, Hefei, Anhui, China*

SUMMARY

Background: **Carbapenem-resistant *Pseudomonas aeruginosa* (CRPA) infection is becoming increasingly severe in clinical practice, yet its host metabolic characteristics remain unclear. Based on metabolomics, this study compares the metabolic profiles of patients infected with CRPA versus susceptible strains, aiming to identify potential diagnostic biomarkers and therapeutic targets.**

Method: **This single-center case-control study enrolled 20 inpatients diagnosed with *Pseudomonas aeruginosa* infection at the Second People's Hospital between May 2023 and May 2024. Based on antimicrobial susceptibility testing, patients were divided into a CRPA group (n = 10) and a carbapenem-susceptible (CSPA) group (n = 10). Plasma samples from all patients underwent untargeted metabolomic analysis using ultrahigh-performance liquid chromatography-mass spectrometry. Differential metabolites were screened by applying principal component analysis, orthogonal partial least squares-discriminant analysis multivariate statistical analysis, and univariate analysis. These metabolites were subsequently annotated and subjected to pathway enrichment analysis using the Kyoto Encyclopedia of Genes and Genomes (KEGG), Human Metabolome Database, and ChemSpider databases.**

Results: **Metabolomic analysis identified 19 differentially abundant metabolites, more than half of which were involved in lipid metabolism. This was primarily characterized by the upregulation of glycerophospholipids (such as phosphatidylserine and phosphatidylinositol) and the downregulation of glycerophosphocholine, phosphatidylethanolamine, and certain sphingolipids. Beyond lipids, compounds such as cholic acids, p-cresol sulfate, and hippuric acid were also significantly upregulated. KEGG enrichment analysis revealed that the differential metabolites were predominantly enriched in pathways related to glycerophospholipid metabolism, sphingolipid metabolism, and ether lipid metabolism, indicating that disrupted lipid metabolism is a core metabolic feature of CRPA infection.**

Conclusions: **This study demonstrates that the metabolic differences in CRPA-infected patients are concentrated in lipid metabolism, suggesting a close association between drug-resistant infections and host-pathogen lipid metabolic remodeling. Changes in relevant lipids hold value as potential diagnostic and prognostic biomarkers, while lipid metabolic pathways may also represent novel targets for future therapeutic interventions.**
(Clin. Lab. 2026;72:xx-xx. DOI: 10.7754/Clin.Lab.2025.250922)

Correspondence:
Xiaoqiong Wang, Yongsheng Wang
Department of Respiratory and Critical Care Medicine
The Second People's Hospital of Hefei
Hefei Hospital Affiliated to Anhui Medical University
Hefei, 230011
Anhui
China

Email: xiaoqiongwang1220@163.com
wangyongshengah@163.com

Manuscript accepted September 29, 2025

KEYWORDS

Pseudomonas aeruginosa, carbapenem resistance, metabolomics, glycerophospholipid metabolism

INTRODUCTION

Carbapenem-resistant *Pseudomonas aeruginosa* (CRPA) is a pathogen associated with serious hospital-acquired infections. In 2017, the World Health Organization classified CRPA as “Priority 1: Critical”, designating it as an antibiotic-resistant "priority pathogen". In the pathogenic spectrum of hospital-acquired pneumonia in China, *Pseudomonas aeruginosa* (PA) accounts for 16.9% - 22.0%, ranking second, and the proportion of PA infection is greater in patients over 65 years of age [1]. Especially in intensive care units, long-term hospitalized patients and immunosuppressed patients, the incidence of PA drug-resistant infections is gradually increasing, which seriously affects patient prognosis [2]. According to the results of China Antimicrobial Surveillance Network in 2024, the resistance rates of PA to imipenem and meropenem were 21.3% and 17.3%, respectively. Although numerous studies have focused on the antibiotic resistance genes, enzymatic mechanisms, and epidemiological characteristics of *Pseudomonas aeruginosa*, there remains limited understanding of the host's metabolic responses during drug-resistant infections.

As a crucial tool in systems biology, metabolomics enables comprehensive detection and analysis of small-molecule metabolites in vivo, providing new insights into host–pathogen interactions during infection. By comparing the metabolic profiles of patients infected with CRPA and carbapenem-susceptible *Pseudomonas aeruginosa* (CSPA), key metabolites and pathways closely associated with drug resistance can be identified. This information holds significant clinical implications: first, in early disease screening, specific aberrant changes in characteristic metabolites may serve as plasma biomarkers for distinguishing between drug-resistant and susceptible infections, offering a rapid and non-invasive diagnostic approach for clinical practice [3]. Second, in risk stratification and prognosis evaluation, changes in the metabolic profile may reflect the severity of inflammation, the intensity of immune response, and clinical outcomes, thereby aiding in the identification of high-risk patients and supporting personalized treatment strategies. Furthermore, the exploration of targeted interventions and novel therapeutics elucidating altered metabolic pathways not only advances our understanding of resistance mechanisms but also reveals potential targets for treatment. Strategies such as modulating host lipid metabolism or intervening in the bile acid–gut microbiota-immune axis could thus emerge as novel therapeutic avenues in the future.

Therefore, this study employed high-resolution untargeted metabolomics technology to investigate serum metabolic alterations in the two groups of patients. These findings could provide a basis for the rational clinical use of medication and infection control by providing insight into the mechanisms of drug resistance and serological characteristics.

MATERIALS AND METHODS

Patients and samples

This study enrolled 20 patients with microbiologically confirmed PA infections who were hospitalized in the Department of Respiratory and Critical Care Medicine at the Guangde Road Branch of Hefei Second People's Hospital between May 2023 and May 2024. Based on antimicrobial susceptibility testing (AST) results and in accordance with the Clinical and Laboratory Standards Institute (CLSI) M100 (33rd edition) guidelines, the patients were divided into two groups: a resistant group (Group R, n = 10), who were infected with CRPA (resistant to imipenem or meropenem), and a susceptible group (Group S, n = 10), who were infected with CSPA.

The inclusion criteria include: 1) Age ≥18 years; 2) Clinically diagnosed respiratory tract infection with microbiologically confirmed *Pseudomonas aeruginosa* infection; 3) Availability of complete clinical and laboratory data; 4) Written informed consent obtained from the patient or their legal representative.

The exclusion criteria include: 1) Coinfection with other pathogens (including other bacteria or fungi) where the exclusive PA infection could not be confirmed; 2) Severe coagulation disorders or ongoing anticoagulant therapy that may compromise blood sample collection; 3) Administration of carbapenem antibiotics within 72 hours prior to enrollment; 4) Pregnancy or lactation; 5) Incomplete clinical data.

Microbiological identification and antimicrobial susceptibility testing

Respiratory specimens, including sputum and bronchoalveolar lavage fluid, were collected from enrolled patients under sterile conditions. The isolated strains were cultured using standard microbiological procedures and identified as Pseudomonas aeruginosa by matrix-assisted laser desorption/ionization time-of-flight mass spectrometry (MALDI-TOF MS; Bruker Daltonics, Germany).

Antimicrobial susceptibility testing (AST) was performed in the clinical microbiology laboratory. The susceptibility results were interpreted according to the Clinical and Laboratory Standards Institute (CLSI) M100 (33rd edition) guidelines. Isolates resistant to imipenem or meropenem were classified as carbapenem-resistant *Pseudomonas aeruginosa* (CRPA), whereas isolates susceptible to both agents were classified as carbapenem-susceptible *Pseudomonas aeruginosa* (CSPA).

Specimen collection

Peripheral venous blood (3 - 5 mL) was collected into K2-EDTA tubes under fasting conditions in the morning. The samples were centrifuged at 3,000 × g for 10 minutes at 4°C to separate plasma. The plasma was aliquoted and stored at -80°C until metabolomic analysis. Prior to analysis, plasma samples were thawed at 4°C and centrifuged at 12,000 × g for 10 minutes to remove debris before metabolite extraction.

Experimental procedures

The collected serum samples were stored at −80°C storage and thawed at 4°C. Aliquots were mixed with pre-chilled methanol/acetonitrile/water (2:2:1, v/v) solution, vortexed, and ultrasonicated for 30 minutes at low temperature. After incubation at -20°C for 10 minutes, the mixture was centrifuged at 14,000 × g (4°C, 20 minutes), and the resulting mixture was lyophilized. Prior to mass spectrometry analysis, the dried extracts were reconstituted in 100 μL of acetonitrile/water (1:1, v/v), vortexed, and centrifuged again (14,000 × g, 4°C, 15 minutes). The final supernatant was transferred for analysis.

Analytical platform

Metabolite separation was performed using an ultra-high-performance liquid chromatography system coupled with a high-resolution mass spectrometer (Q Exactive, Thermo Fisher Scientific, Waltham, MA, USA). Mobile phase A consisted of 0.1% formic acid in water, and mobile phase B was 0.1% formic acid in acetonitrile. The gradient elution program was set to 12 minutes in total, including an initial hold at 95% B, followed by a stepwise gradient decrease to 40% B for separation, and finally re-equilibration to 95% B. The flow rate was set at 0.3 mL/minute, and the column temperature was maintained at 40°C. Samples were kept at 4°C in the autosampler and injected in random order to minimize systematic bias. To ensure system stability and data reproducibility, quality control (QC) samples were inserted at regular intervals (every 10 samples).

Statistical analysis of data

The identified metabolites were annotated using the KEGG database (https://www.genome.jp/kegg/pathway.html), HMDB (https://www.hmdb.ca), and ChemSpider (https://www.chemspider.com) databases.

Following normalization of the metabolomic data using the metaX software, both multivariate and univariate statistical analyses were performed. For multivariate analysis, principal component analysis (PCA) and orthogonal partial least squares discriminant analysis (OPLS-DA) were applied. The stability and significance of the OPLS-DA model were assessed via 7-fold cross-validation and 200 permutation tests. For univariate analysis, differential metabolites between two groups were evaluated using two-sample *t*-tests (or Mann-Whitney U tests for non-normally distributed data), and fold changes (FC, log2-transformed) were calculated. The differential metabolite criteria were VIP > 1, $p < 0.05$, FC > 1.5, or FC < 0.67. Visualization analyses included generating volcano plots using ggplot2 in RStudio. Metabolic pathway enrichment was performed in MetaboAnalyst 5.0. All statistical tests were conducted in SPSS 25.0 with a significance threshold $\alpha = 0.05$ (two-tailed).

RESULTS

Baseline characteristics

The CRPA group comprised 10 patients, including 8 males and 2 females, with ages ranging from 51 to 93 years (mean age: 72.10 ± 14.548 years). The CSPA group also consisted of 10 patients, with 7 males and 3 females, aged between 36 to 94 years (mean age: 70.00 ± 19.788 years). No statistically significant differences were observed between the two groups in terms of age or gender distribution ($p > 0.05$) (Table 1).

Multivariate analysis

As shown in Figure 1, TICs peaks of QC samples exhibited consistent profiles, indicating excellent stability and reproducibility of the analytical platform. In the PCA score plot, the QC samples clustered tightly, further confirming the reliability of the detection system. Although some degree of overlap was observed between the CRPA (Group R) and CSPA (Group S) samples, a distinct separation trend was evident in their metabolic profiles, suggesting differences in plasma metabolomic characteristics between the two patient groups. Further discrimination was performed using the partial least squares-discriminant analysis (PLS-DA) model (Figure 2A). The results revealed a clear separation between the CRPA and CSPA groups in terms of metabolic profiles. The robustness of the model was evaluated through 200 permutation tests (Figure 2B). The intercepts of R^2 and Q^2 were 0.9756 and -0.2103, respectively, indicating high explanatory power and good robustness of the model without overfitting.

Differentially abundant metabolite analysis

A total of 19 differential metabolites were identified through combined multivariate and univariate analysis (VIP > 1.0, $p < 0.05$, FC > 1.5 or < 0.67) (Table 2). Most of these metabolites belonged to glycerophospholipids, including sn-Glycero-3-phosphocholine (GPC), PE 36:1, and Plasmenyl-PC 40:3, which were significantly downregulated in the CRPA group. In contrast, certain phospholipids such as PS 40:8, PS 40:5, and PI 38:4 were markedly upregulated. Additionally, sphingolipids (Cer[NDS] 36:0 and Cer[NS] 38:1) were significantly downregulated in the CRPA group. Beyond lipid metabolism, the steroidal metabolite cholic acid was elevated in the CRPA group. Organic acids and their derivatives, including p-cresol sulfate and hippuric acid, also showed significant increases. Furthermore, the dipeptide Ile-Ala and the nitrogen-containing heterocyclic

Table 1. Baseline demographic characteristics of the CRPA and CSPA groups.

Characteristic	ALL (n = 20)	CSPA (n = 10)	CRPA (n = 10)	p-value
Gender				
Male	15 (75.0%)	7 (70.0%)	8 (80.0%)	
Female	5 (25.0%)	3 (30.0%)	2 (20.0%)	
Age (years)	75.0 (64.8 - 82.5)	74.0 (62.5 - 83.5)	76.0 (67.0 - 79.0)	0.940

Table 2. UPLC-MS/MS-based differentially abundant metabolite identification.

MS2Metabolite	MS2class	ratio	t-test p-value	VIP	regulated
sn-Glycero-3-phosphocholine	glycerophospholipids	0.427	0.005	2.669	down
PS 40:8; PS (20:4/20:4)	glycerophospholipids	1.528	0.005	2.007	up
LysoPE 18:2	glycerophospholipids	0.660	0.007	1.963	down
PE 36:1; PE (18:0/18:1)	glycerophospholipids	0.430	0.009	3.395	down
Plasmenyl-PC 40:3; PC (P-18:0/22:3)	glycerophospholipids	0.319	0.010	3.308	down
p-Cresol sulfate	organic sulfuric acids and derivatives	1.574	0.011	5.047	up
PE (18:0/22:4 (7Z, 10Z, 13Z, 16Z))	glycerophospholipids	0.515	0.015	3.921	down
Ile-Ala	carboxylic acids and derivatives	1.595	0.018	1.963	up
2-Piperidinone	piperidines	2.472	0.020	3.849	up
2-Piperidinone	piperidines	2.226	0.024	3.749	up
Cer [NDS] 36:0; Cer [NDS] (d18:0/18:0)	sphingolipids	0.501	0.027	3.649	down
Cholic acid	steroids and steroid derivatives	4.169	0.027	3.339	up
2,7-Oxepanedione	lactones	0.464	0.029	2.115	down
PS 40:5; PS (18:0/22:5)	glycerophospholipids	2.548	0.033	2.720	up
1-Stearoyl-2-arachidonoyl-sn-glycero-3-phosphoserine	glycerophospholipids	1.655	0.033	3.533	up
PS 36:2; PS (18:0/18:2)	glycerophospholipids	2.313	0.033	3.129	up
Cer [NS] 38:1; Cer [NS] (d18:1/20:0)	sphingolipids	0.468	0.035	2.780	down
PI 38:4; PI (18:0/20:4)	glycerophospholipids	1.626	0.039	3.760	up
Hippuric acid	benzene and substituted derivatives	2.326	0.042	2.316	up

metabolite 2-piperidinone were both upregulated in the CRPA group. Among the 19 differential metabolites, over half (12 metabolites) were associated with lipid metabolic pathways, with glycerophospholipids (10 metabolites) and sphingolipids (2 metabolites) being the predominant classes. These findings suggest that disrupted lipid metabolism is a central feature of the metabolic profile in patients with CRPA infections.

As shown in Figure 3, the volcano plot illustrates the distribution of differential metabolites between the CRPA and CSPA groups. A total of 19 significantly differential metabolites were identified. Among these, 11 metabolites were significantly upregulated in the CRPA group, including PS 40:8, PS 40:5, PS 36:2, PI 38:4, p-cresol sulfate, Ile-Ala, 2-piperidinone, cholic acid, and hippuric acid, and others. The remaining 8 metabolites were significantly downregulated in the CRPA group, including sn-glycero-3-phosphocholine, PE 36:1, plasmenyl-PC 40:3, LysoPE 18:2, PE (18:0/22:4), Cer [NDS] 36:0, Cer[NS] 38:1, and 2,7-oxepanedione.

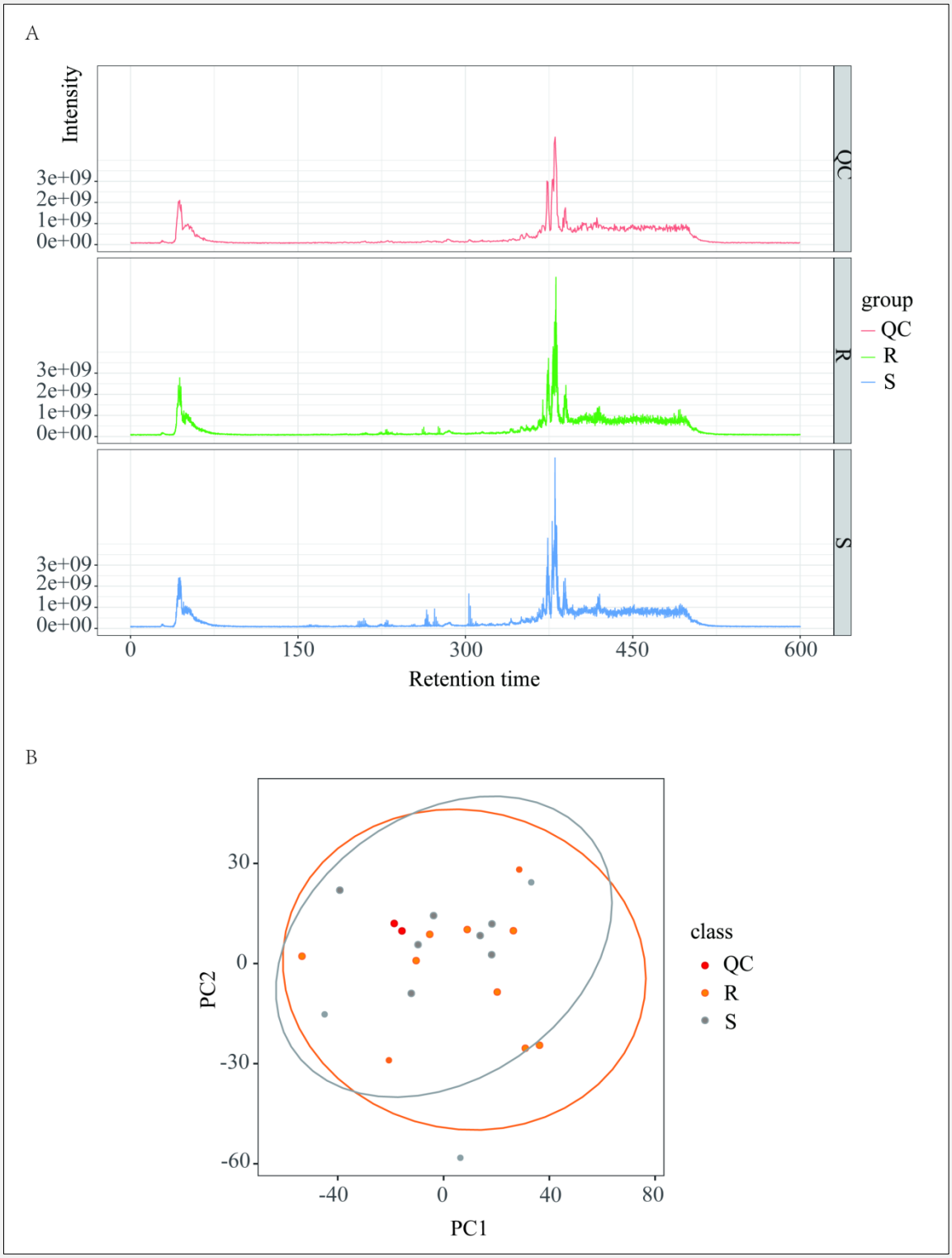

Figure 1A. Total ion chromatograms (TICs) of QC samples and experimental groups.
Figure 1B. PCA scores of the CRPA and CSPA groups.

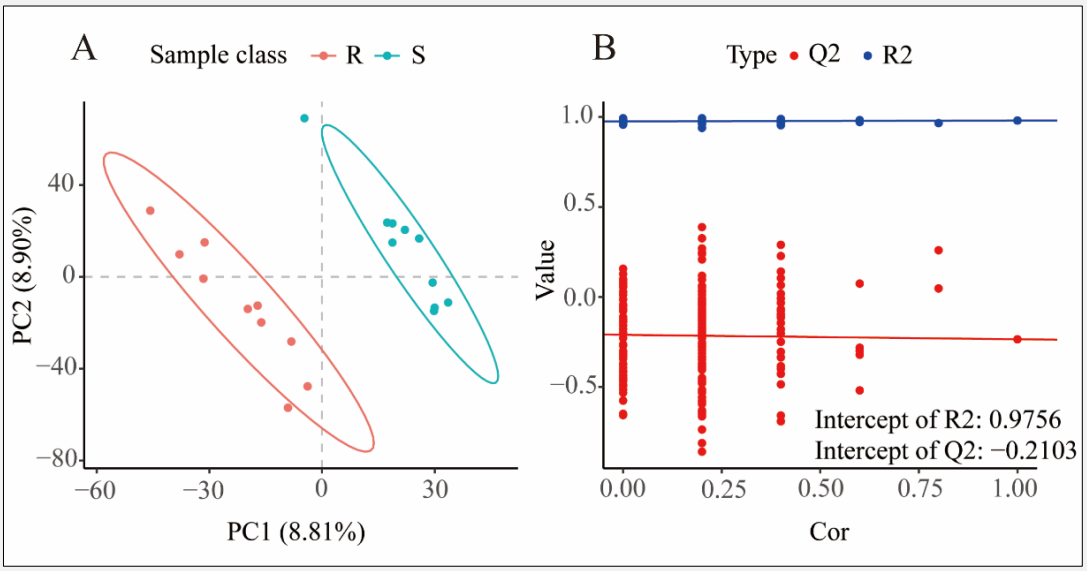

Figure 2. PLSDA scores A) and PLSDA model permutation test plots B) of the CRPA and CSPA groups.

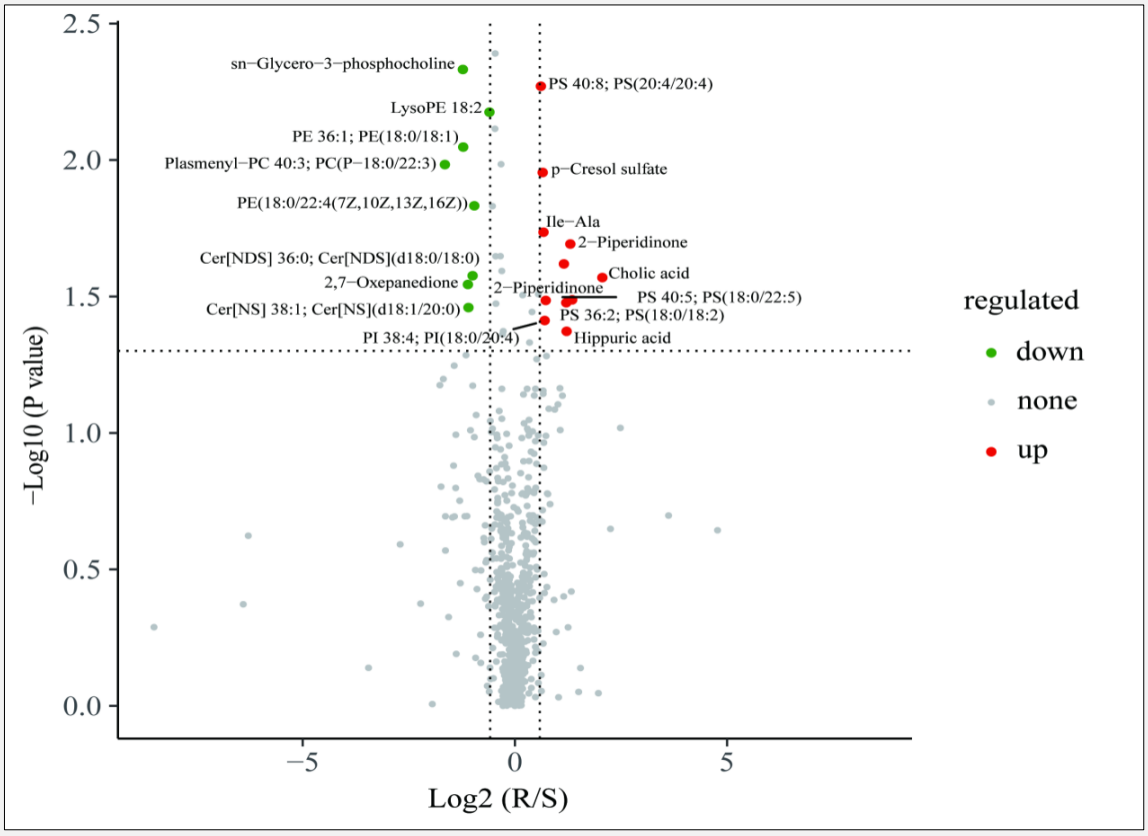

Figure 3. Differentially abundant metabolite volcano plots of the CRPA and CSPA groups.

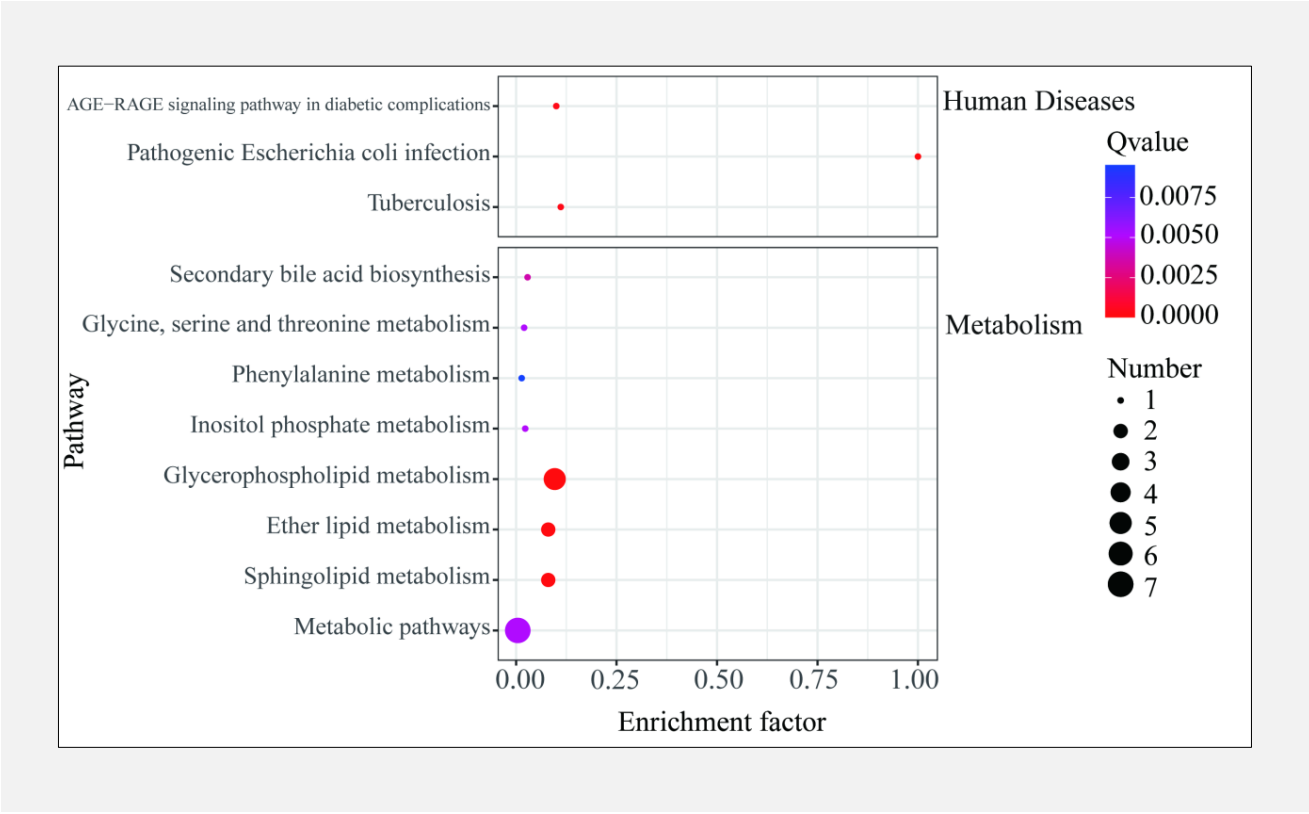

Figure 4. KEGG enrichment of different metabolites in the CRPA and CSPA groups.

Differentially abundant metabolite pathway analysis

As illustrated in Figure 4, KEGG pathway enrichment analysis revealed that the differential metabolites between the CRPA and CSPA groups were primarily enriched in lipid metabolic pathways, including glycerophospholipid metabolism, sphingolipid metabolism, and ether lipid metabolism. Additionally, enrichment was observed in inositol phosphate metabolism and phenylalanine metabolism. Several differential metabolites were also significantly associated with bile acid biosynthesis and amino acid metabolic pathways (such as glycine, serine, and threonine metabolism). In the enrichment bubble plot, pathways such as glycerophospholipid metabolism, sphingolipid metabolism, and ether lipid metabolism were represented by a larger number of bubbles with higher statistical significance (smaller Q-values, indicated by redder colors), suggesting their dominant roles in the metabolic alterations.

DISCUSSION

CRPA has emerged as a global public health threat [4–6]. CRPA infections are associated with suboptimal therapeutic outcomes due to complex resistance mechanisms, including the production of extracellular polysaccharide matrices and resistance to novel β-lactam/β-lactamase inhibitor combinations. These infections are clinically characterized by limited treatment efficacy, high recurrence rates, and substantial economic burden, significantly compromising patient prognosis[7–9]. In this study, we employed high-resolution untargeted metabolomics to compare plasma metabolic profiles between patients with CRPA and CSPA infections. By comparing metabolite profiles and conducting pathway enrichment analysis, we not only revealed alterations in individual metabolites but also elucidated their systemic roles within biological networks [10]. This multi-level approach - from single metabolites to metabolic pathways - provides deeper insights into the systemic metabolic changes induced by resistant infections and offers potential clues for identifying novel therapeutic targets. The observed metabolic alterations in this study were primarily associated with lipid metabolism. Specifically, significant decreases in sn-glycero-3-phosphocholine, phosphatidylethanolamine (PE), and plasmalogens were detected in the CRPA group. sn-glycero-3-phosphocholine (GPC) is a water-soluble metabolite derived from the enzymatic cleavage of host phosphatidylcholine (PC) by phospholipases. In patients with CRPA infection, this metabolic pathway may be attenuated due to the consumption of membrane lipids for emergency membrane repair and antioxidant responses [11]. Furthermore, PA can uptake GPC and convert it into gly-

cine betaine, which further contributes to the depletion of host plasma GPC levels [12,13]. Under infectious stress, rapid turnover of major host membrane lipid components, such as phosphatidylcholine and phosphatidylethanolamine, occurs, accompanied by elevated oxidative stress. This leads to excessive consumption of plasmalogens. Consistent with our findings, studies in septic infection models have also reported significant reductions in plasmalogen levels, which are regarded as metabolic indicators of impaired antioxidant capacity and reduced membrane stability [14]. Phosphatidylethanolamine (PE) is the most abundant phospholipid in bacterial cell membranes. In mammalian cell membranes, it is generally the second most prevalent phospholipid after PC. PE plays a critical role in maintaining membrane fluidity and integrity; a decrease in its levels indicates disrupted lipid homeostasis and impaired energy metabolism. Previous studies have consistently observed reduced PE levels in both human and animal models of sepsis, which is closely associated with adverse outcomes such as immune activation, mitochondrial dysfunction, and immune cell apoptosis [15-17].

In this study, we observed upregulation of PS and PI in the CRPA group. Under physiological conditions, PS is predominantly located on the inner leaflet of the cell membrane. During apoptosis or severe stress, it “flips” to the outer leaflet, aiding in the maintenance of cellular homeostasis [18]. PS can also modulate inflammatory responses by binding to phagocyte receptors [19]. The upregulation of PS in patients with CRPA infection may be attributed to increased apoptotic activity and activation of immune clearance pathways. PI, a major membrane phospholipid, serves as a key substrate for the PI3K/AKT signaling pathway [20]. Accumulating evidence indicates that remodeling of PI is closely associated with inflammatory activation [21]. Therefore, the elevated PI levels observed in CRPA-infected patients likely reflect a high inflammatory state induced by the infection.

In the present study, we observed significantly decreased levels of Cer[NDS] 36:0 and Cer[NS] 38:1 in patients with CRPA. As a central molecule in sphingolipid metabolism, ceramide (Cer) is extensively involved in maintaining cellular membrane structure, regulating inflammatory responses, and modulating apoptosis. Previous studies have indicated that elevated Cer levels in septic patients are associated with an increased risk of mortality [22-25]. However, the alterations in Cer of different chain lengths were not uniform. Cer can significantly influence pathophysiological processes in a chain length-dependent manner [26]. A decrease in certain Cer species may reflect their translocation to membrane pools or conversion into downstream signaling molecules, such as sphingosine-1-phosphate (S1P), thereby contributing to immune responses [27]. In conjunction with our findings, the reduction in specific Cer species in patients with CRPA may suggest that inflammatory and metabolic reprogramming leads to excessive consumption or translocation of particular Cer subspecies. This observation aligns with the high inflammatory burden and immune dysregulation commonly associated with drug-resistant infections.

In the "non-lipid" differential metabolites, the significant elevation of cholic acid suggests that CRPA infection may disrupt the "liver–bile–immune axis." Recent studies indicate that excessive accumulation of bile acids can regulate intestinal barrier function and inflammatory responses via FXR or TGR5 receptors, which, under infectious conditions, are associated with immune imbalance and worsened prognosis [28,29]. Furthermore, p-Cresol sulfate and hippuric acid are both metabolites derived from gut microbiota. Their increased levels in plasma suggest possible gut dysbiosis and intestinal barrier damage, allowing these microbial metabolites to enter systemic circulation and exacerbate systemic inflammatory responses and immune activation [30,31]. This indicates that CRPA infection may also lead to dysregulation of the "liver–gut–immune" crosstalk, amplifying its systemic metabolic and immune burden.

This study has several noteworthy limitations. Firstly, the participant cohort exhibited a relatively high proportion of elderly patients, and the overall sample size was limited. These characteristics may constrain the representativeness and generalizability of the findings to other hospitals or broader regions within the country. Secondly, the detection of PA in this study primarily relied on sputum samples. This reliance on a single specimen source complicates the differentiation between whether the pathogen represents a colonizing strain or a true infecting pathogen. Additionally, the untargeted metabolomics approach has limitations that must be acknowledged. For example, this method struggles to identify numerous unknown metabolites and may be confounded by environmental or food-related contaminants. Furthermore, the non-targeted metabolomics approach carries inherent limitations that must be acknowledged. For instance, current lipid analysis technologies cannot comprehensively detect all lipids in biological samples within a single analytical run; instead, they necessitate the selective combination of multiple analytical techniques for parallel profiling [32]. Finally, some metabolite changes may not be directly caused by PA infection but rather by systemic inflammatory responses or comorbidities.

CONCLUSION

This study revealed that the metabolic differences in patients with CRPA infections are predominantly centered on lipid metabolism, suggesting that drug-resistant infections largely rely on host-pathogen lipid metabolic remodeling and competition. These findings carry dual implications. First, the decrease in specific lipids (such as GPC, plasmalogens, and PE) may serve as potential early diagnostic or prognostic biomarkers. Second, dysregulated lipid metabolism and its associated pathways -

including impaired choline utilization, plasmalogen depletion, and PI3K/AKT signaling activation - represent promising targets for future therapeutic intervention.

Availability of Data and Materials:
The datasets used and/or analyzed during the present study are available from the corresponding authors on reasonable request.

Source of Funds:
This work was supported by Anhui Provincial Key Research Project for Higher Education Disciplines (2024 AH050703), Anhui Provincial Health Research Project (AHWJ2024Ab0233), Applied Medical Research Project of Heifei Municipal Health Commission (Hwk2023 zd012 and Hwk2024zd016), the Science and Technology Project of Bengbu Medical College (2023byzd248).

Declaration of Interest:
The authors have no conflicts of interest to declare.

References:

1. Shi Y, Huang Y, Zhang TT, et al. Chinese guidelines for the diagnosis and treatment of hospital-acquired pneumonia and ventilator-associated pneumonia in adults (2018 edition). J Thorac Dis 2019;11(6):2581-616. (PMID: 31372297)

2. Vincent JL, Sakr Y, Singer M, et al. Prevalence and outcomes of infection among patients in intensive care units in 2017. JAMA 2020;323(15):1478-87. (PMID: 32207816)

3. Johnson CH, Ivanisevic J, Siuzdak G. Metabolomics: beyond biomarkers and towards mechanisms. Nat Rev Mol Cell Biol 2016; 17(7):451-9. (PMID: 26979502)

4. Thaden JT, Park LP, Maskarinec SA, Ruffin F, Fowler VG, Van Duin D. Results from a 13-year prospective cohort study show increased mortality associated with bloodstream infections caused by pseudomonas aeruginosa compared to other bacteria. Antimicrob Agents Chemother 2017;61(6):e02671-16. (PMID: 28373189)

5. Cai B, Echols R, Magee G, et al. Prevalence of carbapenem-resistant gram-negative infections in the United States predominated by acinetobacter baumannii and pseudomonas aeruginosa. Open Forum Infect Dis 2017;4(3):ofx176. (PMID: 29026867)

6. Stewardson AJ, Marimuthu K, Sengupta S, et al. Effect of carbapenem resistance on outcomes of bloodstream infection caused by enterobacteriaceae in low-income and middle-income countries (PANORAMA): a multinational prospective cohort study. Lancet Infect Dis 2019;19(6):601-10. (PMID: 31047852)

7. Cahill ME, Jaworski M, Harcy V, et al. Cluster of Carbapenemase-Producing Carbapenem-Resistant Pseudomonas aeruginosa Among Patients in an Adult Intensive Care Unit - Idaho, 2021-2022. MMWR Morb Mortal Wkly Rep 2023;72(31):844-6. (PMID: 37535466)

8. Labaste F, Grossac J, Bounes FV, et al. Risk factors for acquisition of carbapenem-resistance during treatment with carbapenem in the intensive care unit: a prospective study. Eur J Clin Microbiol Infect Dis 2019;38(11):2077-85. (PMID: 31482416)

9. Qin J, Zou C, Tao J, et al. Carbapenem resistant pseudomonas aeruginosa infections in elderly patients: antimicrobial resistance profiles, risk factors and impact on clinical outcomes. Infect Drug Resist 2022;15:2301-14. (PMID: 35517901)

10. Bauermeister A, Mannochio-Russo H, Costa-Lotufo LV, Jarmusch AK, Dorrestein PC. Mass spectrometry-based metabolomics in microbiome investigations. Nat Rev Microbiol 2022; 20(3):143-60. (PMID: 34552265)

11. Feige E, Mendel I, George J, Yacov N, Harats D. Modified phospholipids as anti-inflammatory compounds. Curr Opin Lipidol 2010;21(6):525-9. (PMID: 20827191)

12. Sun Z, Kang Y, Norris MH, et al. Blocking phosphatidylcholine utilization in pseudomonas aeruginosa, via mutagenesis of fatty acid, glycerol and choline degradation pathways, confirms the importance of this nutrient source *in vivo*. PLoS One 2014;9(7): e103778. (PMID: 25068317)

13. Wargo MJ. Choline catabolism to glycine betaine contributes to pseudomonas aeruginosa survival during murine lung infection. PLoS One 2013;8(2):e56850. (PMID: 23457628)

14. Pike DP, McGuffee RM, Geerling E, et al. Plasmalogen loss in sepsis and SARS-CoV-2 infection. Front Cell Dev Biol 2022;10: 912880. (PMID: 35784479)

15. Tasseva G, Bai HD, Davidescu M, Haromy A, Michelakis E, Vance JE. Phosphatidylethanolamine deficiency in mammalian mitochondria impairs oxidative phosphorylation and alters mitochondrial morphology. J Biol Chem 2013;288(6):4158-73. (PMID: 23250747)

16. Liu H, Li Z, Zhang X, Zhao JC, Chai J, Chang C. Multi-omics reveals aberrant phenotypes of respiratory microbiome and phospholipidomics associated with asthma-related inflammation. Microorganisms 2025;13(8):1761. (PMID: 40871265)

17. Schoeler M, Caesar R. Dietary lipids, gut microbiota and lipid metabolism. Rev Endocr Metab Disord 2019;20(4):461-72. (PMID: 31707624)

18. Fadok VA, Voelker DR, Campbell PA, Cohen JJ, Bratton DL, Henson PM. Exposure of phosphatidylserine on the surface of apoptotic lymphocytes triggers specific recognition and removal by macrophages. J Immunol 1992;148(7):2207-16. (PMID: 1545126)

19. Birge RB, Boeltz S, Kumar S, et al. Phosphatidylserine is a global immunosuppressive signal in efferocytosis, infectious disease, and cancer. Cell Death Differ 2016;23(6):962-78. (PMID: 26915293)

20. Guo Y, Yu Y. PI3K/Akt pathway and neuroinflammation in sepsis-associated encephalopathy. Open Med (Wars) 2025;20(1): 20251248. (PMID: 40823184)

21. Chaudhry H, Zarban AA, Trevelin SC, et al. Phosphatidylinositol-4,5-bisphosphate 3-kinase (PI3K) inhibitors reduce vascular inflammation *in vitro* and *in vivo*. Br J Pharmacol Epub August 18, 2025. (PMID: 40826960)

22. Wu X, Hou J, Li H, et al. Inverse correlation between plasma sphingosine-1-phosphate and ceramide concentrations in septic patients and their utility in predicting mortality. Shock 2019; 51(6):718-24. (PMID: 30080743)

23. Coant N, Sakamoto W, Mao C, Hannun YA. Ceramidases, roles in sphingolipid metabolism and in health and disease. Adv Biol Regul 2017;63:122-31. (PMID: 27771292)

24. Winkler MS, Nierhaus A, Poppe A, Greiwe G, Gräler MH, Daum G. Sphingosine-1-phosphate: a potential biomarker and therapeutic target for endothelial dysfunction and sepsis? Shock 2017; 47(6):666-72. (PMID: 27922551)

25. Tanaka A, Honda T, Yasue M, et al. Effects of ceramide kinase knockout on lipopolysaccharide-treated sepsis-model mice: changes in serum cytokine/chemokine levels and increased lethality. J Pharmacol Sci 2022;150(1):1-8. (PMID: 35926944)

26. Grösch S, Schiffmann S, Geisslinger G. Chain length-specific properties of ceramides. Prog Lipid Res 2012;51(1):50-62. (PMID: 22133871)

27. Kuo A, Hla T. Regulation of cellular and systemic sphingolipid homeostasis. Nat Rev Mol Cell Biol 2024;25(10):802-21. (PMID: 38890457)

28. Qian S, Su Z, Lin J, et al. Inhibition of farnesoid-x-receptor signaling during abdominal sepsis by dysbiosis exacerbates gut barrier dysfunction. Cell Commun Signal 2025;23(1):236. (PMID: 40399878)

29. Godlewska U, Bulanda E, Wypych TP. Bile acids in immunity: bidirectional mediators between the host and the microbiota. Front Immunol 2022;13:949033. (PMID: 36052074)

30. Shiba T, Makino I, Kawakami K, Kato I, Kobayashi T, Kaneko K. p-cresyl sulfate suppresses lipopolysaccharide-induced antibacterial immune responses in murine macrophages *in vitro*. Toxicol Lett 2016;245:24-30. (PMID: 26784855)

31. Mirji G, Bhat SA, El Sayed M, et al. Aromatic microbial metabolite hippuric acid potentiates pro-inflammatory responses in macrophages through TLR-MyD88 signaling and lipid remodeling. bioRxiv (Preprint) 2025;2025.05.19.654724. (PMID: 40475494)

32. Hornburg D, Wu S, Moqri M, et al. Dynamic lipidome alterations associated with human health, disease and ageing. Nat Metab 2023;5(9):1578-94. (PMID: 37697054)